The final publication is available at

http://doi.org/10.1039/c5cy02298c

Additional Information

Improving the catalytic performance of SAPO-18 for Methanol-to-Olefins (MTO) by controlling the Si distribution and crystal size

Raquel Martínez-Franco,[1] Zhibin Li,[1,2] Joaquín Martínez-Triguero,[1] Manuel Moliner,[1]* Avelino Corma[1]*

[1] Instituto de Tecnología Química (UPV-CSIC), Universidad Politécnica de Valencia, Consejo Superior de Investigaciones Científicas, Valencia, 46022, Spain

[2] School of Chemistry and Materials Science, Heilongjiang University, Harbin 150080, China

*Corresponding authors: E-mail addresses: acorma@itq.upv.es; mmoliner@itq.upv.es

Abstract

The physico-chemical properties of the small pore SAPO-18 zeotype have been controlled by properly selecting the organic molecules acting as organic structure directing agents (OSDAs). The two organic molecules selected to attempt the synthesis of the SAPO-18 materials were N,N-diisopropylethylamine (DIPEA) and N,N-dimethyl-3,5-dimethylpiperidinium (DMDMP). On one hand, DIPEA allows achieving small crystal sizes (0.1-0.3 μm) with limited silicon distributions when the silicon content in the synthesis gel is high (Si/TO$_2$ ~ 0.8). On the other hand, the use of DMDMP directs the formation of larger crystallites (0.9-1.0 μm) with excellent silicon distributions, even when the silicon content in the synthesis media is high (Si/TO$_2$ ~ 0.8). It is worth noting that this is the first description of the use of DMDMP as OSDA for the synthesis of the SAPO-18 material, revealing not only the excellent directing role of this OSDA to stabilize the large cavities present in the SAPO-18 structure, but also to selectively place the silicon atoms in isolated framework positions. The synthesized SAPO-18 materials have been characterized by different techniques, such as powder X-ray diffraction (PXRD), scanning electron microscopy (SEM), N$_2$ adsorption, solid NMR, or ammonia temperature programmed desorption (NH$_3$-TPD). Finally, their catalytic activity has been evaluated for the Methanol-to-Olefin (MTO) process at different reaction temperatures (350 and 400ºC), revealing that the SAPO-18 catalysts with optimized silicon distributions and crystal sizes show excellent catalytic properties for the MTO reaction. These optimized SAPO-18 materials present improved catalyst lifetimes compared to standard SAPO-34 and SSZ-39 catalysts, even when tested at low reaction temperatures (i.e. 350ºC).

1.- Introduction

The Methanol-to-Olefins (MTO) process has received a significant attention in the last years since it has been considered as an alternative route for the production of light olefins, such as ethylene and propylene, which are currently mainly achieved from fluid catalytic cracking or steam cracking of hydrocarbons.[1,2]

Small pore silicoaluminophosphate (SAPO) materials containing large cavities in their structures, have been described as the most efficient catalysts for the MTO reaction.[2,3] Indeed, SAPO-34 material, which is the silicoaluminophosphate form of the crystalline structure of CHA,[4] is being applied as commercial catalyst for this process.[3,5] It is claimed that the unique crystalline structure of CHA, combining the presence of large cavities (~ 6.7x10.9 Å) and small pores (~ 3.8 Å), allows the formation of the required bulky aromatic intermediate states, known as "hydrocarbon pool", and permits the preferential diffusion of the desired light olefins, respectively.[6,7,8,9,10]

In addition to the SAPO-34 catalyst, other small pore SAPO materials presenting large cavities in their structure have also been studied as catalysts for the MTO process.[11,12] From the different SAPO materials, SAPO-18 has shown remarkable catalytic activities for the MTO reaction and high selectivities towards desired light olefins.[13,14,15,16] SAPO-18 has the AEI framework topology, and its crystalline structure is highly related to CHA, presenting the same framework density (FD ~ 15.1 T atoms/1000Å^3), and similar three-dimensional small pore systems.[17] However, the zeolitic cages present in the AEI and CHA structures show different shape, being the AEI cage basket-shaped and wider at the bottom than the CHA cage (see Figure 1).

The different shape of the AEI cavities may influence the formation of the bulky aromatic intermediates, and consequently, the product selectivities to light olefins.[18] Indeed, recent descriptions have shown that AEI structures tend to produce more propylene and less ethylene than CHA catalysts,[19,20] which is interesting owing to the higher rate in the demand of propene.

Unfortunately, only few reports can be found in the literature dealing with the synthesis and optimization of the SAPO-18 material.[17,21] In fact, most of the reported syntheses for the SAPO-18 material are referred to the former method described by Chen et al., where N,N-diisopropylethylamine (DIPEA) is used as organic structure directing agent (OSDA).[17] This methodology allows synthesizing SAPO-18 materials

with limited silicon distributions, detecting the formation of large amounts of agglomerated silicon species within the crystals.[17] It is worth noting that the silicon-rich domains are formed by the multiple substitution of P^{5+} and Al^{4+} atoms in the zeolitic framework by Si^{4+} atoms, resulting in materials with lower Brønsted acidities and hydrothermal stabilities.

In general, the presence of weaker Brønsted acidities on small pore SAPO catalysts tends to decrease the catalyst deactivation rate for the MTO process,[22] but in contrast, higher reaction temperatures (i.e. 400ºC) are required to afford total methanol conversions compared to aluminosilicate counterparts.[23,24] In this sense, it could be expected that the improvement of the Brønsted acid properties of SAPO-18 materials by optimizing their silicon distributions may allow operating the industrial MTO process at lower reaction temperatures (i.e. 350ºC), resulting in a significant enhancement of the catalyst lifetimes. Thus, the efficient preparation of the SAPO-18 material with the adequate physico-chemical properties could result in a competitive catalyst for the MTO.

Very recently, we have described for the first time the use of cyclic ammonium cations, such as N,N-dimethyl-3,5-dimethylpiperidinium (DMDMP), as OSDAs for the efficient direct synthesis of Cu-containing SAPO-18 catalysts for DeNOx applications.[25] The combination of DMDMP and a Cu-complex in the synthesis media, not only has allowed improving the crystallization of the Cu-SAPO-18 material, but also selectively placing the silicon and copper species in isolated framework positions and extra-framework cations, respectively.[25] A plausible explanation for the better Cu-SAPO-18 crystallization when using DMDMP as OSDA compared to the traditional DIPEA molecule could be found in the superior specificity of the cyclic ammonium cations towards the large cavity present within the AEI structure.[26] If this is so, it could be expected that the use of the DMDMP as OSDA in absence of Cu-complexes, would also influence the nucleation of the metal-free SAPO-18 materials, and consequently, their silicon distribution and acid properties, especially for Si-rich SAPO-18 materials.

Herein, we describe the preparation of different SAPO-18 materials with diverse and controlled silicon distributions and different crystal sizes, by properly selecting the organic molecule used as OSDA (DIPEA or DMDMP, see Figure 2). The resultant SAPO-18 materials have been characterized and their catalytic activity evaluated for the MTO

process at two different reaction temperatures (350 and 400ºC). It has been observed that the SAPO-18 materials with optimized silicon distributions and crystal sizes show excellent catalytic properties for the MTO process, achieving longer catalyst lifetimes than a standard SAPO-34 catalyst or the corresponding aluminosilicate counterparts, as SSZ-39 materials. It is especially remarkable the excellent catalytic behavior of the optimized SAPO-18 material when the reaction is performed at lower temperature (350ºC). This introduces a stable SAPO-based catalyst that is very attractive for the industrial MTO process.

2.- Experimental Section

2.1.- Syntheses

2.1.1.- N,N-dimethyl-3,5-dimethylpiperidinium (DMDMP) synthesis

10 g of 3,5-dimethylpiperidine (C_7H_{15}, Acros Organics, 96%, cis-trans mixture) was mixed with 140 ml of methanol (CH_3OH, Scharlab, 99.9%) and 19.51 g of potassium carbonate ($KHCO_3$, Sigma Aldrich, 99.7%). Later, 54 ml of methyl iodide (CH_3I, Sigma Aldrich, 99.9%) was added dropwise, and the resultant mixture maintained under stirring for 7 days. After this period, the mixture was filtered to remove most of the potassium bicarbonate, and the solution washed several times with chloroform. The combined organic extracts were dried over $MgSO_4$, filtered and finally, the quaternary ammonium salt (85% yield) was precipitated with diethyl ether. The iodide salt was converted to the hydroxide salt by treatment with a hydroxide anion-exchange resin (Dowex SBR).

2.1.2.- Zeotype synthesis

- **SAPO-18 materials**

In a typical zeotype synthesis procedure, the required amount of orthophosphoric acid (85%wt, Aldrich) was first mixed with the corresponding OSDA [N,N-dimethyl-3,5-dimethylpiperidinium (DMDMP), or N,N-diisopropylethylamine (DIPEA)]. Second, the required amount of the aluminum source (alumina, 75%wt, Condea) was added, keeping the gel under stirring for 5 minutes. Finally, the required amount of a silica source (Ludox AS40, 40%wt, Aldrich) was introduced into the synthesis gel, leaving the mixture under stirring for 20 minutes. The gel was transferred to a Teflon-lined

stainless steel autoclave with a free volume of 3 ml, and heated at 190ºC under rotation for 12 hours. The synthesis conditions for the different SAPO-18 materials are summarized in Table 1. After the crystallization procedure, the crystalline products were filtered and washed with abundant water, and dried at 100ºC overnight. The samples were calcined at 550ºC in air for 4 hours to properly remove the occluded organic species.

- **SAPO-34 material**

In a typical synthesis of SAPO-34, the required amount of an aqueous solution of tetraethylammonium (TEAOH, 35 %wt Sigma-Aldrich) hydroxide was mixed with the required amount of distilled water and phosphoric acid (85 %wt, Aldrich). This mixture was stirred for 30 min. Secondly, the required content of alumina (75 %wt, Condea) and silica (Ludox AS40 40%wt, Aldrich) was introduced in the above mixture, and the resultant gel was stirred until complete homogenization. The chemical composition of the synthesis gel was $0.18\ SiO_2 : 0.5\ Al_2O_3 : 0.4\ P_2O_5 : 0.9\ TEAOH : 18\ H_2O$. The crystallization was conducted at 200°C for 1 day under dynamic conditions. The solid product was filtered and washed with abundant water and dried at 100°C. The crystalline sample was calcined at 550°C in air to remove the occluded organic species.

2.2.- Characterization

The crystallinity of the solids was characterized by powder X-ray diffraction (PXRD) using a multisample Philips X`Pert diffractometer equipped with a graphite monochromator, operating at 40 kV and 45 mA, and using Cu K_α radiation (λ= 0.1542 nm).

The chemical analyses were carried out in a Varian 715-ES ICP-Optical Emission spectrometer, after solid dissolution in an aqueous solution of $HNO_3/HCl/HF$ solution.

The morphology and particle size of the materials were studied by field emission scanning electron microscopy (FESEM) using a ZEISS Ultra-55 microscope.

Textural properties (BET surface area and micropore volume) were determined by N_2 adsorption isotherms measured at 77 K with a Micromeritics ASAP 2020.

The ^{29}Si MAS NMR spectra were recorded at room temperature using a Bruker AV 400 spectrometer MAS, with a spinning rate of 5 kHz at 79.459 MHz a 55° pulse length of 3.5 μs and repetition time of 180 s. ^{29}Si chemical shift was referred to tetramethylsilane.

NH_3-TPD experiments were carried out in a Micromeritics 2900 apparatus. A calcined sample (100 mg) was activated by heating to 400°C for 2 h in an oxygen flow and for 2 h in argon flow. Subsequently, the samples were cooled down to 176°C, and NH_3 was adsorbed. The NH_3 desorption was monitored with a quadrupole mass spectrometer (Balzers, Thermo Star GSD 300T) while the temperature of the sample was ramped at 10°C min^{-1} in helium flow. Total ammonia adsorption was measured by repeated injection of calibrated amounts of ammonia at 100°C until saturation. Ammonia desorption was recorded by means of the mass 15, since this mass is less affected by the desorbed water.

2.3.- Catalytic experiments

The catalyst was pelletized, crushed and sieved into 0.2-0.4 mm particle size. 50 mg of sample was mixed with 2 g quartz (Fluka) before being introduced into the fixed-bed reactor (7mm diameter). N_2 (30mL/min or 19 mL/min) was bubbled in methanol hold at (-17°C or 25.5°C), giving a WHSV of 0.8 h^{-1} or 7h^{-1}, respectively. The catalyst was first activated with an air flow of 80 ml/min for 1 h at 540°C, and then the temperature was decreased to reaction conditions (350°C or 400ºC, respectively). Each experiment was analyzed every 5 minutes with an online gas chromatograph (Bruker 450GC, with PONA and Al_2O_3-Plot capillary columns, and two FID detectors). After reaction, the catalyst was regenerated at 540°C in 80ml of air for 3h and the reaction was repeated again. Preliminary experiments were carried out at constant WHSV, different amount of catalyst and increasing flow rates, and later with catalyst with in different particle sizes, to check that, at the selected reaction conditions the process is not controlled by either external or intra-particle diffusion. Conversion and selectivities were considered in carbon basis and methanol and dimethylether were lumped together for calculation of conversion.

3.- Results

3.1.- Zeolite synthesis and characterization

The SAPO-18 synthesis has been attempted using two different organic molecules, such as DIPEA and DMDMP (see Figure 2), and two different silicon contents [Si/(Al+P) = 0.05 and 0.08] were selected for each OSDA (see SAPO-18_1 to _4 in Table 1). The entire synthesis conditions for these four experiments are summarized in Table 1, where it could be remarked that the synthesis gels were concentrated [H_2O/(Al+P) ratio ~ 5], and the zeotype crystallizations were carried out at 190ºC for 12 hours under dynamic conditions.

The PXRD patterns of the achieved solids confirm the formation of pure SAPO-18 materials (see SAPO-18_1 to _4 in Figure 3). However, the PXRD patterns of the SAPO-18_1 and _2, which have been synthesized in presence of DIPEA as OSDA, show less intense and wider diffraction peaks compared to SAPO-18_3 and _4, which have been synthesized using DMDMP (see Figure 3). These results may reveal different crystal morphologies for the SAPO-18 depending on the OSDA used in their preparation. Indeed, the study of these samples by field emission scanning electron spectroscopy (FE-SEM) confirms their different morphology and crystal sizes (see Figure 4). SAPO-18_1 and _2 samples are formed by the aggregation of small crystals with sizes in the range between 100 to 300 nm, while SAPO-18_3 and _4 samples are formed by larger cubic crystals with sizes ranging from 0.7-1.0 μm (see Figure 4).

These as-prepared SAPO-18 materials have been calcined in air at 550ºC to remove the organic species occluded within the crystalline structures and, the calcined SAPO-18 samples have been characterized by N_2 adsorption to study their textural properties. As it can be observed in Table 2, all the calcined SAPO-18 samples show similar BET surface area and micropore volume (~500-520 m^2/g, and ~0.24-0.25 cm^3/g, respectively) but, as expected, the SAPO-18 samples with smaller crystal sizes show larger external surface areas (~30-40 m^2/g, see SAPO-18_1 and _2 in Table 2).

ICP analyses have been performed on the SAPO-18 samples to elucidate their final chemical composition. As seen in Table 3, the amount of Si in the crystalline SAPO-18 materials can be controlled [Si/TO_2 ~ 0.065 and 0.08], depending on the initial Si content introduced in the synthesis gels [Si/(Al+P) ~ 0.05 and 0.08, respectively, see Table 1]. From these chemical analyses, it could be stated that the different OSDAs are not influencing the incorporation of the overall amount of silicon species in the final

SAPO-18 materials, since the measured Si/TO_2 ratios are comparable regardless the OSDA used (see Table 3).

The silicon distribution within the different SAPO-18 materials has been studied by solid ^{29}Si MAS NMR spectroscopy (see Figure 5). The ^{29}Si MAS NMR spectrum of SAPO-18_1 material reveals four clear bands centered at -93, -98, -102 and -112 ppm, corresponding to the presence of Si(4Al) [isolated Si atoms], Si(3Al), Si(Al) and Si(0Al) [silicon islands] environments, respectively (see SAPO-18_1 in Figure 5). This ^{29}Si MAS NMR spectrum indicates that the synthesis of the Si-rich SAPO-18 material using DIPEA as OSDA results in a SAPO catalyst, where almost 50% of the Si species are agglomerated under different Si environments. Similar Si distributions have been described in the literature for the SAPO-18 materials synthesized using DIPEA as OSDA.[17] However, if the Si content is decreased for the preparation of the SAPO-18 using DIPEA, it can observed that the amount of Si species forming agglomerated Si environments are notoriously reduced (see ^{29}Si MAS NMR spectrum of SAPO-18_2 in Figure 5), improving the overall Si distribution as isolated species. On the other hand, the ^{29}Si MAS NMR spectra of the two SAPO-18 materials synthesized using DMDMP as OSDA, exhibit the presence of a single peak centered at -93 ppm (see SAPO-18_3 and _4 in Figure 5). This result indicates that all silicon atoms are selectively replacing phosphorous atoms within the SAPO-18 framework when DMDMP is used as OSDA, regardless the Si content introduced in the samples. That means that the cyclic ammonium DMDMP cation is a very efficient OSDA not only to crystallize the SAPO-18 structure, but also to selectively place the Si atoms in isolated environments.

The different silicon distributions observed within the SAPO-18 samples suggest that these materials should present different acid properties. Thus, the calcined SAPO-18 materials have been characterized by temperature-programmed desorption of ammonia (NH_3-TPD). As it can be seen in Figure S1, the SAPO-18 samples show the presence of different ammonia desorption peaks at different temperatures. The first peak centered at 180ºC has been assigned to weak acid sites corresponding to P-OH hydroxyl groups,[27] and the peaks centered at 375ºC and 425 would indicate the presence of medium and strong acid sites, respectively, which would correspond to the acidic protons associated with the presence of isolated silicon species in the zeolitic framework.[27] The quantification of the desorbed ammonia for the Si-rich

SAPO-18 materials [Si/TO$_2$ ~0.08, see Table 3], reveals that the SAPO-18_1 sample shows higher concentration of weak acid sites (0.16 mmol NH$_3$/g) and less concentration of medium-strong acid sites (0.35 + 0 mmol NH$_3$/g) than the SAPO-18_3 sample (0.11, and 0.49 + 0.22 mmol NH$_3$/g, respectively, see Table 3). The different silicon distributions observed for both SAPO-18 materials would mostly explain these different NH$_3$-TPD profiles, since the higher amount of agglomerated silicon species within the framework of the SAPO-18_1 sample (~50%) would favor the presence of weak acid sites, while hindering the medium-strong acid sites. On the other hand, the quantification of the desorbed ammonia peaks for the SAPO-18 materials synthesized with lower Si content [Si/TO$_2$~ 0.066, see Table 3], reveals that both samples show similar amount of weak acid sites (0.07-0.09 mmol NH$_3$/g), but the SAPO-18_4 presents higher medium-strong acid sites (0.29 + 0.15 mmol NH$_3$/g) than the SAPO-18_2 (0.33 + 0 mmol NH$_3$/g, see Table 3). Since both SAPO-18 samples show comparable silicon distribution (see Figure 5) and Si content (see Table 3), the superior amount of desorbed ammonia at high temperatures observed for the SAPO-18_4 sample, could be mainly related with the presence of larger diffusion paths within the large crystal sizes of the SAPO-18_4 (see Figure 4).[28]

For comparison purposes, a standard SAPO-34 catalyst has been prepared under similar synthesis conditions than those used for the SAPO-18 materials (see Table 1). The PXRD pattern of this material reveals the formation of the crystalline structure of CHA (see SAPO-34 in Figure 3), and FE-SEM spectroscopy shows the formation of crystals with an average size of 0.4-0.5 µm (see SAPO-34 in Figure 4). ICP analysis gives a Si/TO$_2$ molar ratio for SAPO-34 of 0.10 (see Table 3), and the ^{29}Si MAS NMR spectrum indicates the presence of a mixture of silicon environments, most of them as isolated silicon species (see signal centered at ~ -93 ppm, see Figure 5). Finally, NH$_3$-TPD shows that SAPO-34 presents medium and strong Brønsted acid sites, with similar measured values to those obtained for the SAPO-18_4 (see Table 3).

3.2.- Catalytic activity

- *Study of the catalytic activity of SAPO materials for the MTO process at 400ºC*

SAPO-based catalysts are mainly tested in the literature for the MTO reaction at high temperatures (~400ºC) to favor the total conversion of methanol due to its lower

Brønsted acidity compared to zeolites. Having that in mind, the catalytic activity of the different SAPO-18 and SAPO-34 materials have been first studied for the MTO reaction at 400ºC and WHSV=7 h^{-1} (see experimental section). As it can be seen in Figure 6, all the tested materials reached 100% initial methanol conversions, with catalyst lifetimes between 185 and 235 minutes (measured as the time required to achieve 50% methanol conversions, X_{50}).

The material showing the fastest catalyst deactivation is the SAPO-18_3, which presents a methanol conversion drop below 50% after 185 minutes on stream (see Figure 6). The faster catalyst deactivation profile of SAPO-18_3 at 400ºC compared to the other SAPO materials can be explained by its larger crystal sizes (~ 1 μm, see Table 2) and higher acidity (see Table 3), which favors the coke formation by increasing the mass transfer restrictions and the undesired oligomerization of the formed light olefins, respectively.

The other three SAPO-18 materials present comparable catalyst lifetimes, observing that the drop of methanol conversion to below 50% is obtained after ~220-235 minutes on stream (see Figure 6), the small differences between them could be attributed to differences in physico-chemical properties. In this sense, the SAPO-18_1, which has the lowest crystal sizes combined with low-medium acidity (see Tables 2 and 3), shows the highest catalyst lifetime (X_{50} = 235 min) when performing the MTO reaction at 400ºC. On the other hand, SAPO-18_2 and _4 catalysts show almost identical X_{50} catalyst lifetime (X_{50} = 230 min, see Figure 6), which could be attributed to their intermediate Brønsted acidity (see Table 3). However, if their entire methanol conversion profiles are analyzed, it can be observed that SAPO-18_4 is able to fully convert methanol for longer time than SAPO-18_2 (~ 125 and 60, respectively) but, in contrast, SAPO-18_4 shows a steeper catalyst deactivation than SAPO-18_4 (see the slope for the methanol conversion drop for SAPO-18_2 and _4 catalysts in Figure 6). The appearance of steeper methanol conversion drops can be mainly associated to catalysts with large crystal sizes, as it is the case of the SAPO-18_4 material (~ 1 μm, see Table 2).

The catalytic behavior of the SAPO-18 materials for the MTO reaction at 400ºC has been compared with a standard SAPO-34 material (see Figure 6). SAPO-34 shows a similar methanol conversion profile to SAPO-18 catalysts, achieving a 50% methanol

conversion after 220 minutes, which is equivalent to the X_{50} values obtained for the SAPO-18_2 and _4 catalysts (see Figure 6). These analogous catalyst lifetimes could be explained by their comparable acidities, especially for SAPO-18_4 and SAPO-34 materials (see Table 3), and by the intermediate crystal size of SAPO-34 (see Table 2).

Regarding the selectivity to products when the MTO reaction is undergone at 400ºC, SAPO-18 materials show higher selectivities to propylene and butylenes, and lower to ethylene than the standard SAPO-34 catalyst at high methanol conversions (C2= 24-25% vs 35%; C3= 46-48% vs 43%; C4= 21-24% vs 17%, for the SAPO-18 and SAPO-34 materials, respectively, see Figure 7). Indeed, the $C2^=/C3^=$ ratio is much higher for SAPO-34 than for the diverse SAPO-18 materials at different methanol conversions (see Figure S2-left), while the C4/C3 ratio is remarkably higher for the SAPO-18 materials (see Figure S2-right). These differences on the product selectivies between SAPO-34 and SAPO-18 catalysts could be attributed to the different shape of the larges cavities present in both materials (see Figure 1).[19,29] The larger size of the AEI cage within the SAPO-18 materials could favor the formation of "hydrocarbon pool" intermediates with the adequate size to increase the selectivity to propylene and butylenes.[19]

The hydrogen transfer indexes (HTI), measured as C2/C2=, C3/C3=, and C4/C4=, are summarized for the different SAPO materials tested at 400ºC in Figure S3. In general, it can be observed that the initial HTI values tend to be higher for SAPO-18 (see Figure S3). The reason of that is because the hydrocarbon pool aromatic species would be mainly formed when the MTO reaction starts, favoring the presence of cyclization reactions and hydrogen transfer to olefin precursors, increasing the formation of paraffins. After the hydrocarbon pools have been formed within most of the zeolitic cages, the successive cyclization reactions on the aromatic species would result in their progressive growth and, consequently, catalyst deactivation. As it can be seen in Figure S3, SAPO-18_3 and SAPO-18_4 catalysts show higher HTI values compared to the other SAPO materials, especially at high TOS, which could be explained by their larger crystal sizes (~ 1 µm, see Table 2), in clear accordance with their faster catalyst deactivation.

- *Study of the catalytic activity of SAPO materials for the MTO process at 350ºC*

The MTO results achieved at 400ºC for the different SAPO-18 materials are significant, since these materials show high initial catalytic activity, achieving 100% methanol

conversions, with comparable catalyst lifetimes to well-stablished SAPO-34 catalysts. At this point, and since there is a remarkable industrial interest in operating the MTO process at lower temperatures, the above catalysts were studied at 350ºC. We expect that at lower temperatures, the differences on the physico-chemical properties of the SAPO-18 catalysts, such as crystal sizes and Brønsted acidity, would considerably influence their catalytic activity and deactivation. It is worth noting that the MTO experiments at 350ºC have been performed at WHSV=0.8 h^{-1}, to compare the catalytic activity results of these SAPO materials with previous related catalysts that have been studied within our group.

As can be seen in Figure 8a, all the SAPO-18 materials are able to almost achieve complete methanol conversions. Nevertheless, a short initial induction period is observed, especially for SAPO-18_3 and _4, which present higher crystal sizes (~ 1 µm, see Table 3). Interestingly, the SAPO-18 materials show significant catalytic differences when tested at 350ºC, especially different deactivation profiles with time on stream.

The two SAPO-18 samples synthesized with the highest Si content (Si/TO$_2$ ~ 0.08, see Table 3), have the lowest catalyst lifetimes at 350ºC (X$_{50}$ values of 370 and 546 minutes for SAPO-18_1 and SAPO-18_3, respectively, see Figure 8a). The relatively low catalyst lifetime observed for the SAPO-18_3 sample could be related to its high crystal sizes and high Brønsted acidity (see Tables 2 and 3). However, the particular low catalyst lifetime observed for the SAPO-48_1 is not fully understood at the moment, since this catalyst shows relatively low crystal sizes with medium Brønsted acidity, and a better catalyst stability against deactivation by coke formation should be expected (see Tables 3 and 4). Some authors have suggested that the presence of some extend of silicon islands (see the band centered at -112 ppm in the ^{29}Si MAS NMR spectum of the SAPO-18_1 in Figure 5) in the SAPO catalysts could favor the catalyst deactivation, since some of the silicon species present at the borders of the silicon islands could present higher acidities, resulting in a faster rate of coke formation.[2,28] Nevertheless, further studies are required to properly understand this unexpected deactivation behavior observed for the SAPO-18_1 catalyst at 350ºC.

On the other hand, SAPO-18_2 and SAPO-18_4 catalysts, both synthesized with lower Si contents (Si/TO$_2$ ~ 0.06, see Table 3), show remarkably higher X$_{50}$ values at 350ºC, requiring 1040 and 840 minutes to achieve a methanol conversion drop below 50%,

respectively (see Figure 8a). Since these two SAPO-18 materials show comparable silicon content (see Table 2), and in both cases, almost all the silicon species are present as isolated species (see ^{29}Si MAS NMR spectra in Figure 5), their different crystal sizes can mainly explain their different catalytic lifetime (note that SAPO-18_2 and SAPO-18_4 show average crystal sizes of 0.1-0.2 and 0.9-1.0, respectively, see Figure 4). It appears then that introducing the proper amount of Si atoms in isolated form [Si(4Al)], and controlling the size of the crystallites, is the direction to go for achieving SAPO-18 materials able to work satisfactory at lower temperatures (i.e. 350ºC).

A standard SAPO-34 material has also been tested at 350ºC to compare its catalytic activity with that of the SAPO-18 materials. This material shows a similar methanol conversion profile to the one observed for the SAPO-18_4 catalyst, presenting both catalysts an identical X_{50} value (~ 840 minutes, see Figure 8a). This is not surprising since both contain similar crystal sizes and Brønsted acidities (see Tables 2 and 3).

The different SAPO-18 materials tested at 350ºC show comparable product selectivities towards the desired olefins at methanol conversion values above 90%, providing nearly 25%, 48% and 20% for ethylene, propylene, and butylene, respectively (see SAPO-18_1 to _4 in Figure 9). On the other hand, the product selectivities achieved with the SAPO-34 catalyst are significantly different, providing nearly 33%, 46%, and 15% for ethylene, propylene, and butylene, respectively (see SAPO-34 in Figure 9). In general, it can be observed that SAPO-18 and SAPO-34 materials give similar selectivities to propylene, but SAPO-18 materials provide higher amount of butylene and less of ethylene than SAPO-34. Consequently, the $C2^=/C3^=$ ratio is substantially higher for SAPO-34, and the $C4^=/C3^=$ ratio is much higher for SAPO-18 materials (see Figure S4). As it has been hypothesized above, the larger size of the AEI cage present in the SAPO-18 materials could favor the formation of propylene and butylene.[19]

The hydrogen transfer indexes (HTI) of the SAPO catalysts tested at 350ºC are summarized in Figure S5. As expected, SAPO-18_1 and SAPO-18_2, both presenting small crystal sizes (~0.1 μm, see Figure 4), show much lower HTI values than the other SAPO-18 and SAPO-34 catalysts (see Figure S5).

- *Comparison of the catalytic activity of SAPO-18 materials with related aluminosilicates (SSZ-39)*

Very recently, the synthesis of the aluminosilicate form of the AEI structure, SSZ-39 zeolite, has been described in their nanosized form (~50 nm).[20,30] This material has been tested for the MTO reaction at 350ºC and WHSV=0.8 h^{-1}, obtaining an excellent catalytic activity and catalyst lifetime (X_{50}=860 min, see SSZ-39_50 nm in Figure 8b). This nanosized SSZ-39 clearly improves the catalytic properties of the standard SSZ-39, which presents larger crystal sizes (~500 nm), resulting in a faster catalyst deactivation (X_{50}=530 min, see SSZ-39_50 nm in Figure 8b).[20]

If the catalytic activity achieved with these SSZ-39 zeolites for the MTO process at 350ºC is compared with the obtained using the optimized SAPO-18 catalysts, it can be observed that SAPO-18_2 presents lower deactivation with longer catalyst lifetime than both SSZ-39 materials (X_{50} = 1040 min, see Figure 8b), while SAPO-18_4 catalyst shows comparable catalyst lifetime to the obtained with the nanocrystalline SSZ-39 catalyst (X_{50} = 840 min, see Figure 8b). The explanation for the remarkable lower catalyst deactivation achieved for the SAPO-18, particularly for the SAPO-18_2 sample, compared to SSZ-39 catalysts, even when the former zeotypes show higher crystal sizes, could be found in the lower density of strong acid sites present in the SAPO materials (see Table 3).

Thus, these results clearly indicate that the preparation of new polymorphs of small-pore silicoaluminophosphates, containing controlled Brönsted acidities with well-distributed Si species, and adequate crystal sizes,[31] allows achieving competitive catalysts for the MTO reaction, even when the MTO process is performed at low reaction temperatures (i.e. 350ºC).

4.- Conclusions

Different synthesis variables, including the OSDA and silicon content, have been studied in order to synthesize diverse SAPO-18 materials with controlled silicon distributions and crystal sizes. The SAPO-18 materials obtained using N,N-diisopropylethylamine (DIPEA) as OSDA present smaller crystal sizes (~ 0.1-0.3 µm) than those obtained using N,N-dimethyl-3,5-dimethylpiperidinium (DMDMP, ~ 0.7-1.0 µm). On the other hand, DIPEA allows limited silicon distributions when the silicon

content in the synthesis gel is high (Si/TO$_2$ ~ 0.8), while the use of DMDMP results in excellent silicon distributions, even when the silicon content in the synthesis media is high (Si/TO$_2$ ~ 0.8).   The catalytic activity of these SAPO-18 materials has been evaluated for the Methanol-to-Olefin (MTO) process at different reaction temperatures (350 and 400ºC). The SAPO-18 catalysts presenting optimized Si distributions and crystal sizes show longer catalyst lifetimes than a standard SAPO-34 or the silicoaluminate SSZ-39 material, even when the MTO reaction is carried out at low temperature (i.e. 350ºC).

Figure 1: Cavities of the CHA (a) and AEI (b) structures
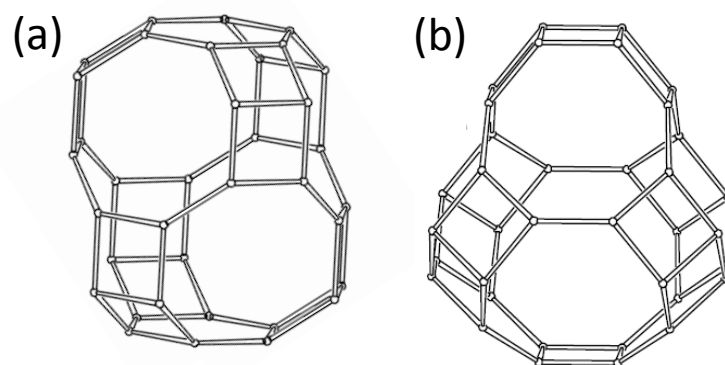
Figure 2: Organic structure directing agents used for the synthesis of SAPO-18 materials: (a) N,N-diisopropylethylamine (DIPEA), and (b) N,N-dimethyl-3,5-dimethylpiperidinium (DMDMP)
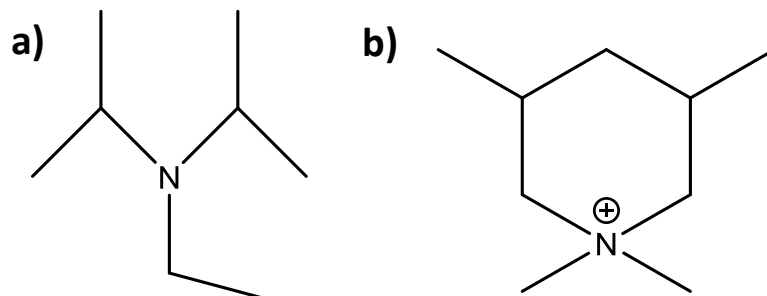
a)

b)

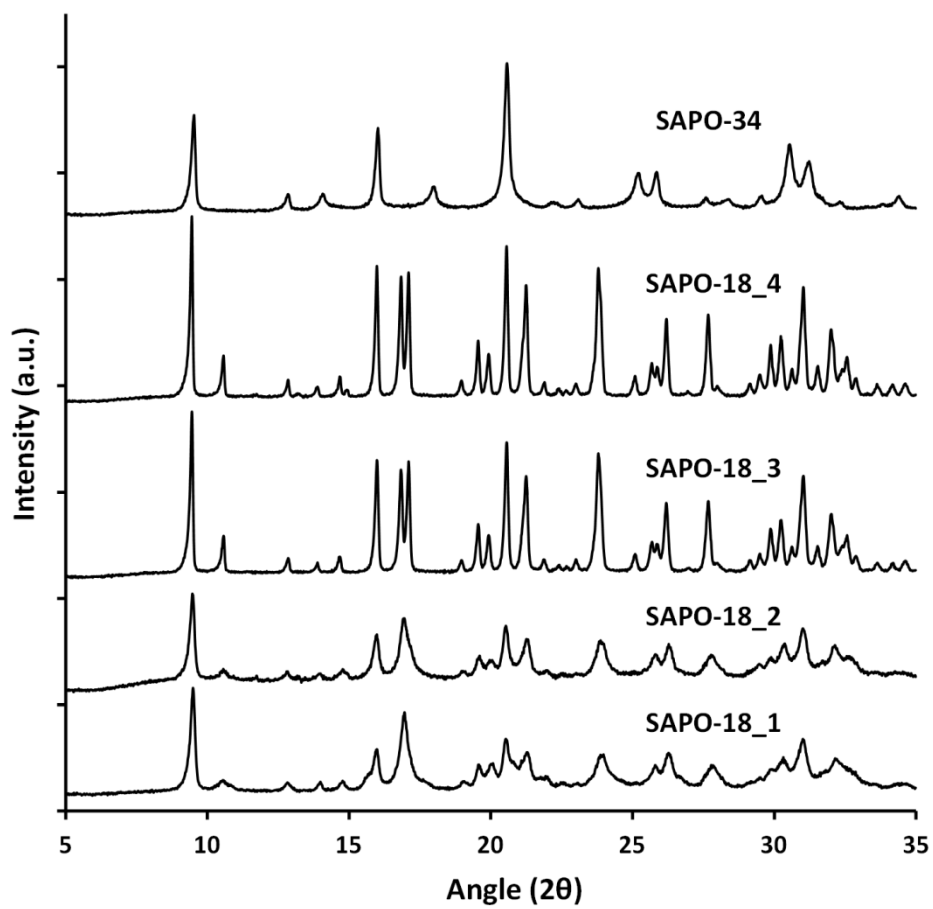**Figure 3: PXRD patterns of the as-synthesized SAPO-18 materials**
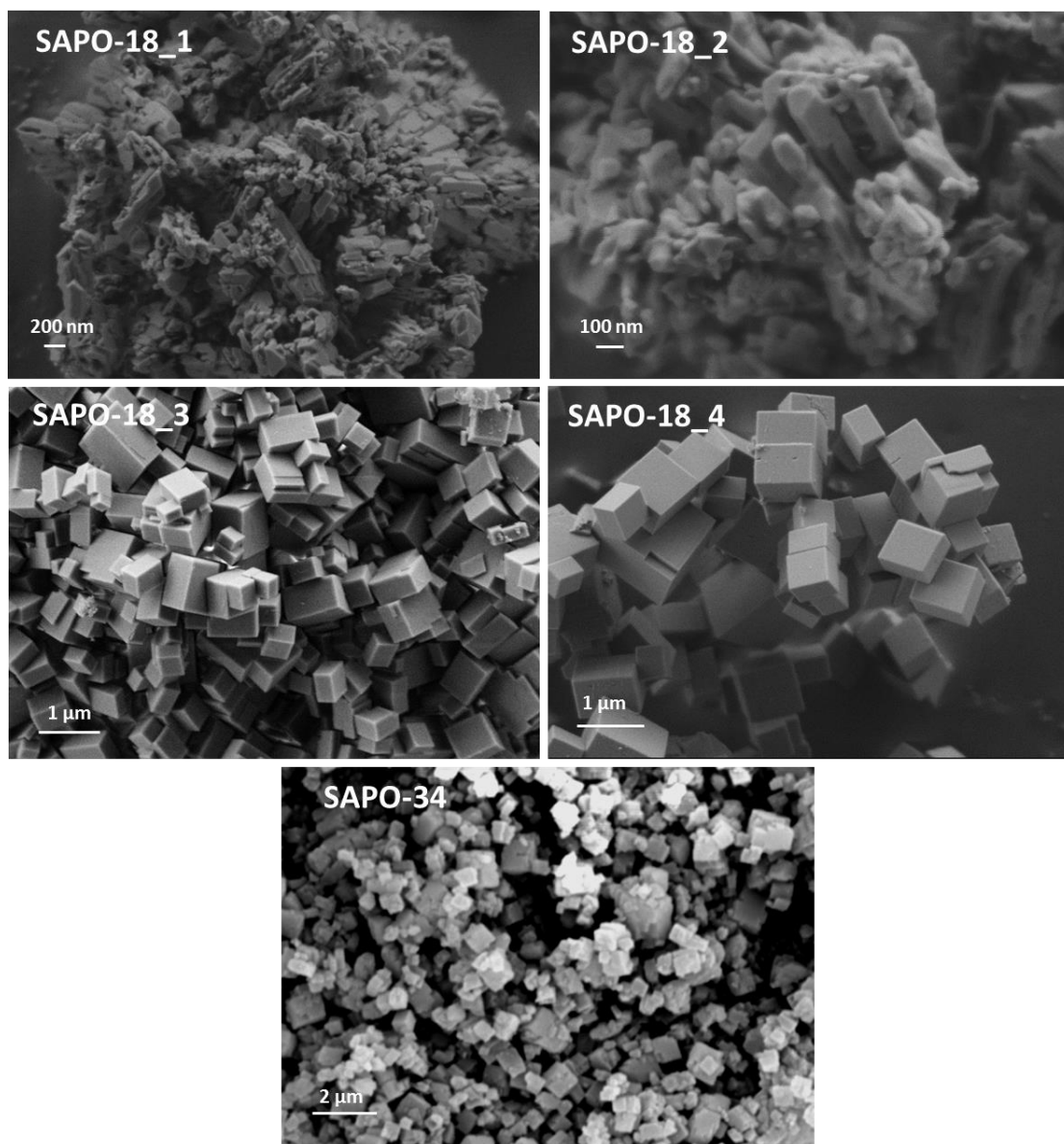
Figure 4: FE-SEM images of the SAPO-18 and SAPO-34 materials

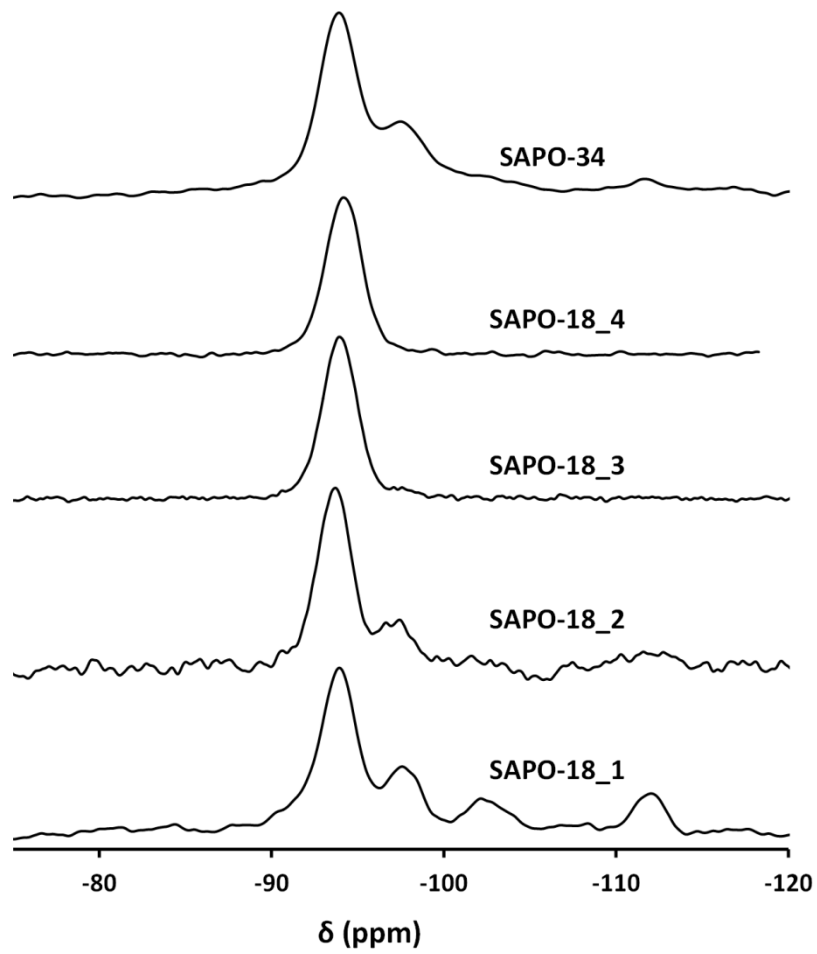**Figure 5:** ^{29}Si MAS NMR of calcined SAPO-18 and SAPO-34 materials

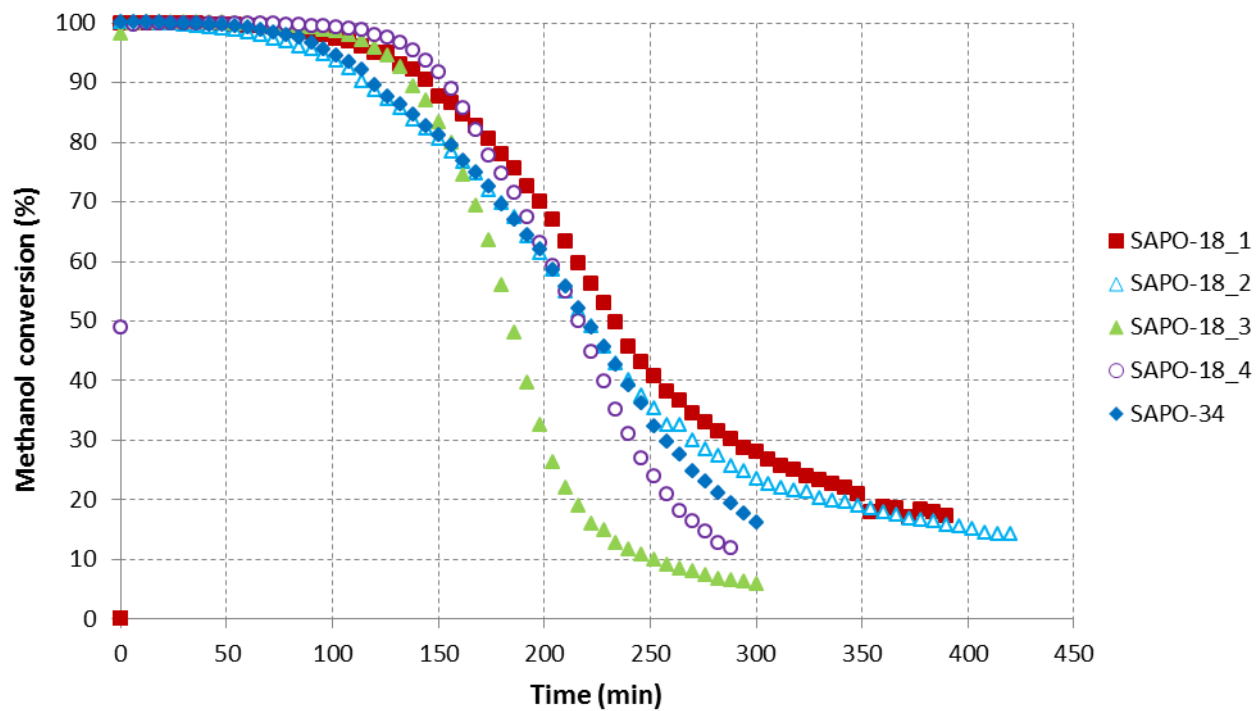**Figure 6: Methanol conversion at 400°C and WHSV=7 h^{-1} for the SAPO-18 and SAPO-34 materials**

Figure 7: Selectivities to C2, C3, C4 and C5+ hydrocarbons at different methanol conversions when testing the SAPO catalysts at 400ºC
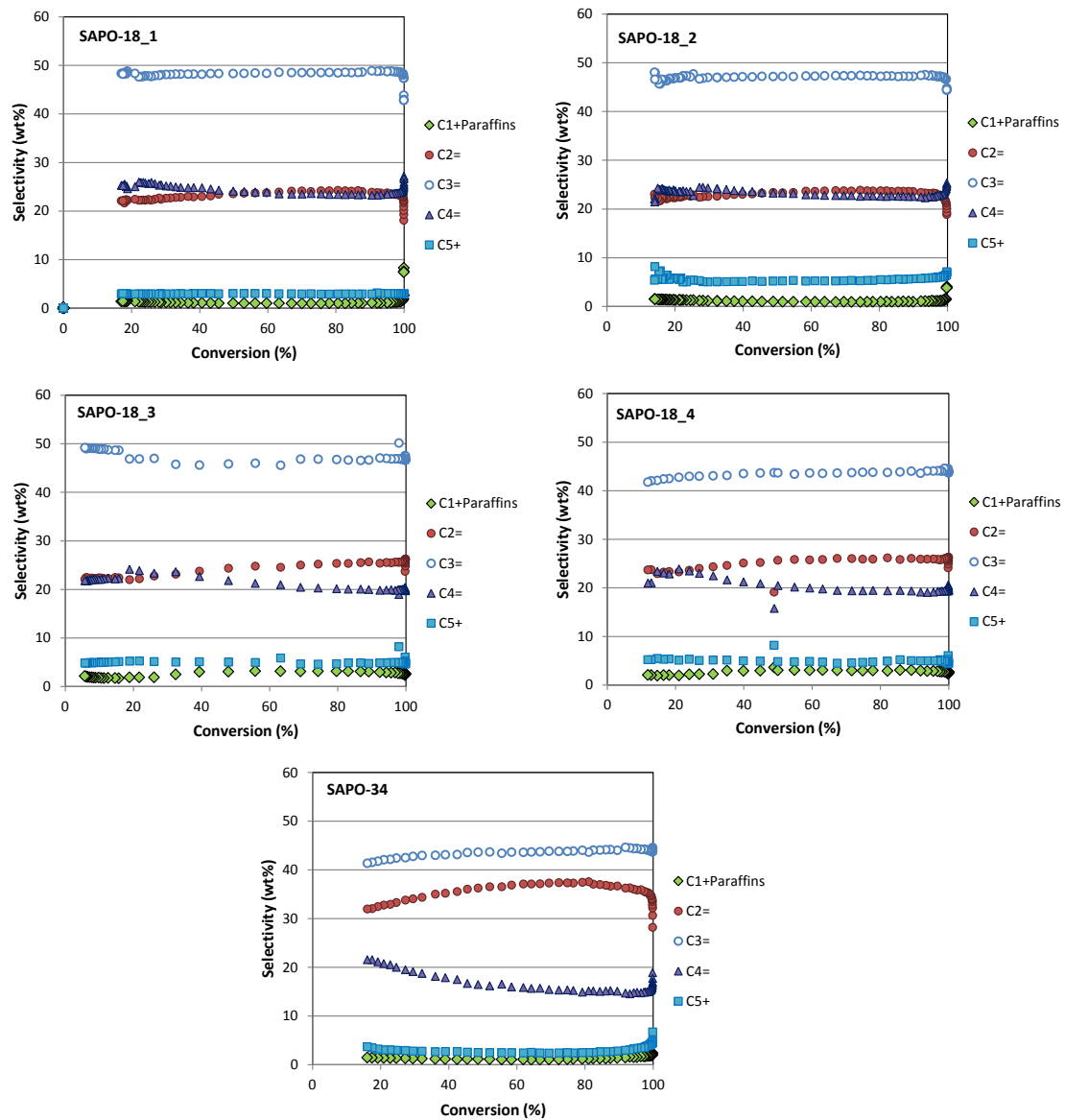
Figure 8: Methanol conversion at 350°C and WHSV=0.8 h^{-1} for the SAPO-18 and SAPO-34 materials (a) and SAPO-18 and SSZ-39 materials (b)
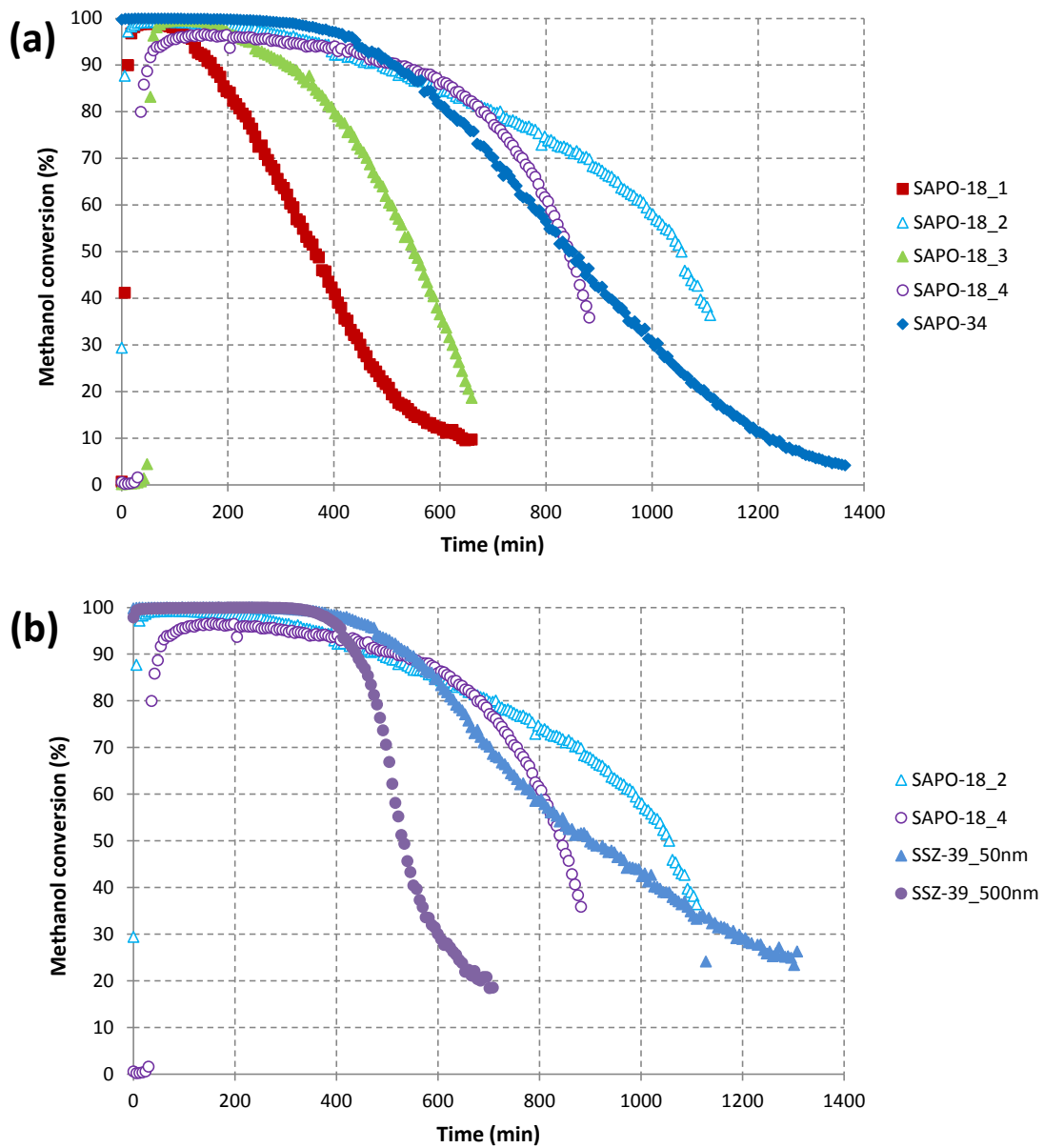
Figure 9: Selectivities to C2, C3, C4 and C5+ hydrocarbons at different methanol conversions when testing the SAPO catalysts at 350ºC
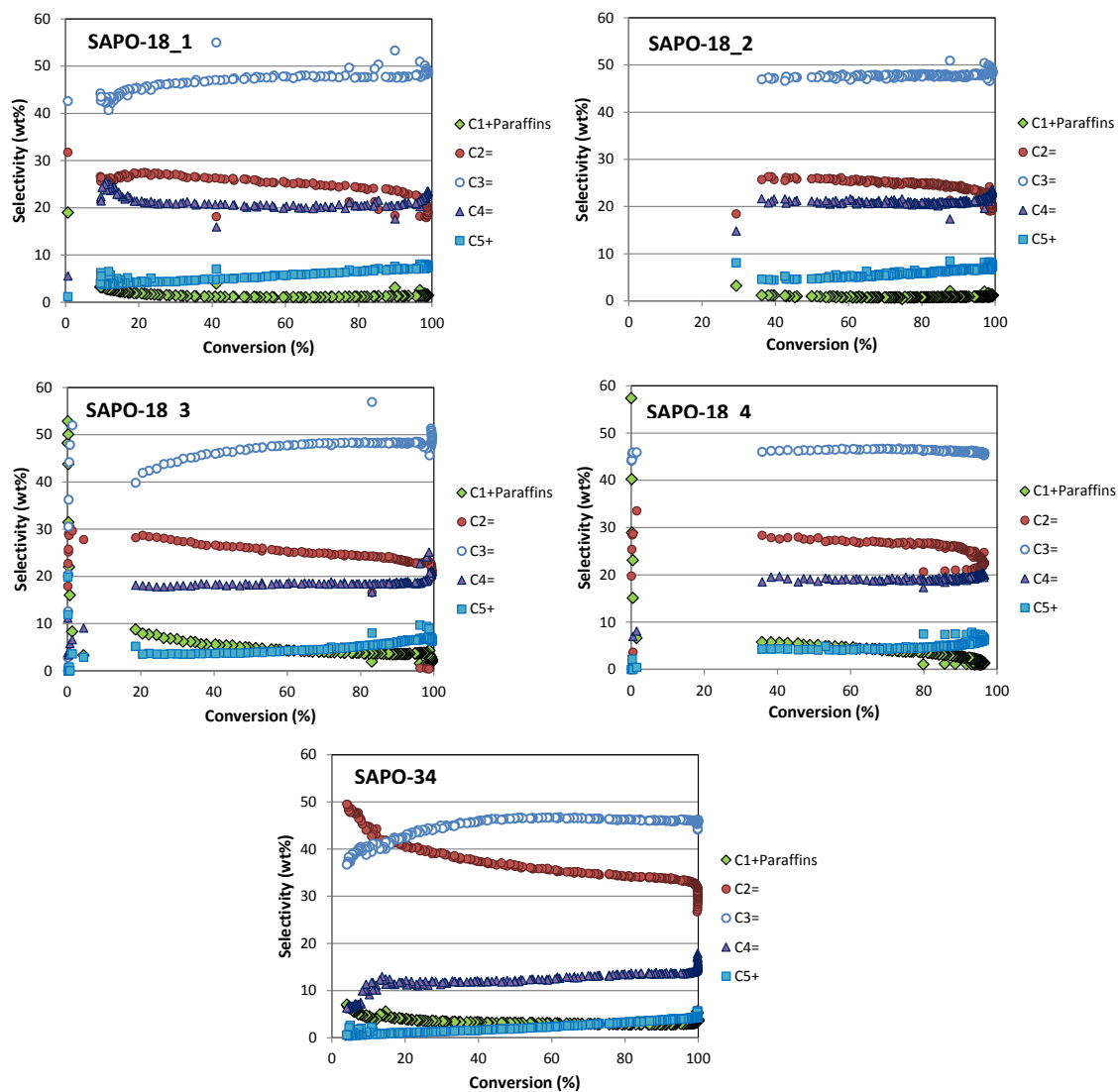
Table 1: Molar ratios used for the synthesis of each SAPO-18 materials

Sample	OSDA	P/Al	Si/Al	Si/(Al+P)	OSDA/(Al+P)	H_2O/(Al+P)
SAPO-18_1[a]	DIPEA	0.85	0.15	0.08	0.5	5
SAPO-18_2[a]	DIPEA	0.9	0.1	0.05	0.5	5
SAPO-18_3[a]	DMDMP	0.85	0.15	0.08	0.3	5
SAPO-18_4[a]	DMDMP	0.9	0.1	0.05	0.3	5
SAPO-34[b]	TEA	0.8	0.2	0.10	0.5	10

[a] All SAPO-18 materials were crystallized at 190ºC for 12 hours, [b] SAPO-34 was crystallized at 200ºC for 24 hours

Table 2: Textural properties of the SAPO-18 materials

Sample	Crystal size (µm)	BET (m^2/g)	A_{micro} (m^2/g)	A_{Ext} (m^2/g)	V_{micro} (cm^3/g)
SAPO-18_1	0.1-0.2	534	494	39	0.24
SAPO-18_2	0.1-0.3	503	479	23	0.23
SAPO-18_3	0.7-0.9	522	515	7	0.25
SAPO-18_4	0.9-1.0	493	491	2	0.24
SAPO-34	0.5	475	454	21	0.26

Table 3: Chemical analyses and acid strength of the SAPO-18 materials

| Sample | Si/TO$_2$^{a} | P/TO$_2$^{a} | Al/TO$_2$^{a} | Acidity (mmol NH$_3$/g) | | | |
				Weak	Medium	Strong	Total
SAPO-18_1	0.08	0.41	0.51	0.16	0.35	---	0.51
SAPO-18_2	0.07	0.41	0.52	0.07	0.33	---	0.40
SAPO-18_3	0.08	0.40	0.52	0.11	0.49	0.22	0.82
SAPO-18_4	0.07	0.40	0.53	0.09	0.29	0.15	0.53
SAPO-34	0.09	0.36	0.54	0.10	0.35	0.18	0.63
SSZ-39_50nm	0.12 (Al/Si)	---	---	---	---	0.49	0.49
SSZ-39_500nm	0.12 (Al/Si)	---	---	---	---	0.54	0.54

^{a} Where T= P + Si+ Al

References:

[1] D. Chen, K. Moljord, A. Holmen; Microporous Mesoporous Mater., 164 (2012) 239-250.

[2] P. Tian, Y. Wei, M. Ye, Z. Liu; ACS Catalysis, 5 (2015) 1922-1938.

[3] M. Moliner, C. Martínez, A. Corma; Chem. Mater., 26 (2014).

[4] B. M. Lok, C. A. Messina, R. L. Patton, R. T. Gajek, T. R. Cannan, E. M. Flanigen; J. Am. Chem. Soc., 106 (1984) 692-693.

[5] J. Q. Chen, A. Bozzano, B. Glover, T. Fuglerud, S. Kvisle; Catal. Today, 106 (2005) 103-107.

[6] M. Stöcker; Microporous Mesoporous Mater, 29 (1999) 3-48.

[7] M. Stöcker; Zeolites and Catalysis, Wiley-VCH Verlag GmbH & Co. KGaA, 2010, 687-711.

[8] B.P.C. Hereijgers, F. Bleken, M.H. Nilsen, S. Svelle, K.P. Lillerud, M. Bjørgen, B.M. Weckhuysen, U. Olsbye; J. Catal., 264 (2009) 77-87.

[9] W. Song, J.F. Haw, J.B. Nicholas, C.S. Heneghan; J. Am. Chem. Soc., 122 (2000) 10726-10727.

[10] S. Wilson, P. Barger; Micropor. Mesopor. Mater., 29 (1999) 117-126.

[11] W. Dai, X. Wang, G. Wu, N. Guan, M. Hunger, L. Li; ACS Catal., 1 (2011) 292-299.

[12] M. A. Deimund, J. E. Schmidt, M. E. Davis; Top. Catal., 58 (2015) 416-423.

[13] R. Wendelbo, D. Akporiaye, A. Andersen, I. M. Dahl, H. B. Mostad; Appl. Catal. A., 142 (1996) L197-L207.

[14] A. G. Gayubo, A. T. Aguayo, A. Alonso, J. Bilbao; Ind.Eng.Chem.Res, 46 (2007) 1981-1989.

[15] J. Chen, J. Li, Y. Wei, C. Yuan, B. Li, S. Xu, Y. Zhou, J. Wang, M. Zhang, Z. Liu; Catal. Commun., 46 (2014) 36-40.

[16] T. Álvaro-Muñoz, C. Márquez-Álvarez, E. Sastre, Top. Catal., 2015, DOI 10.1007/s11244-015-0447-0.

[17] J. Chen, P. A. Wright, J. M. Thomas, S. Natarajan, L. Marchese, M. Bradley, G. Sankar, C. R. A. Catlow; J.Phys. Chem., 98 (1994) 10216.

[18] Y. Bhawe, M. Moliner-Marin, J. D. Lunn, Y. Liu, A. Malek, M. E. Davis; ACS Catal., 2 (2012) 2490.

[19] M. Dusselier, M. A. Deimund, J. E. Schmidt, M. E. Davis; ACS Catal., 5 (2015) 6078–6085.

[20] N. Martín, Z. Li, J. Martínez-Triguero, J. Yu, M. Moliner, A. Corma; Chem. Commun., submitted.

[21] (a) J. Chen, J. M. Thomas, P. A. Wright; Catal. Lett., 28 (1994) 241-284; (b) M. Hunger, M. Seiler, A. Buchholz; Catal. Lett.,74 (2011) 61-68; (c) D. Fan, P. Tian, S. Xu, Q. Xia, X. Su, L. Zhang, Y. Zhang, Y. He, Z. Liu; Mater. Chem., 22 (2012) 6568-6574; (d) S. Abdollahi, M. Ghavipour, M. Nazari, R. M. Behbahani, G. R. Moradi; J. Nat. Gas Sci. Eng., 22 (2015) 245-251.

[22] L.-T. Yuen, S. I. Zones, T. V. Harris, E. J. Gallegos, A. Auroux, Microporous Mater. 2 (1994) 105.

[23] F. Bleken, M. Bjørgen, L. Palumbo, S. Bordiga, S. Svelle, K.P. Lillerud, U. Olsbye, Top. Catal. 52 (2009) 218.

[24] L. Wu, V. Degirmenci, P. C. M. M. Magusin, N. J. H. G. M. Lousberg, E. J. M. Hensen, J. Catal. 298 (2013) 27–40.

[25] R. Martínez-Franco, M. Moliner, A. Corma; J. Catal., 319 (2014) 36-43

[26] P. Wagner, Y. Nakagawa, G. S. Lee, M. E. Davis, S. Elomari, R. C. Medrud, S. I. Zones; J.Am.Chem.Soc., 122 (2000) 263-273.

[27] T. Yu, J. Wang, M. Shen, W. Li; Catal. Sci. Technol., 3 (2013) 3234-3241.

[28] N. Katada, K. Nouno, J. K. Lee, J. Shin, S. B. Hong, M. Niwa; J. Phys. Chem. C, 115 (2011) 22505-22513.

[29] R. L. Smith, S. Svelle, P. del Campo, T. Fuglerud, B. Arstad, A. Lind, S. Chavan, M. P. Attfield, D. Akporiaye, M. W. Anderson; Appl. Catal. A-Gen, 505 (2015) 1.

[30] N. Martín, C. R. Burundea, M. Moliner, A. Corma; Chem. Commun., 51 (2015) 11030-11033.

[31] (a) M. V. Opanasenko, W. J. Roth, J. Cejka; Catal. Sci. Technol. (2016), DOI: 10.1039/C5CY02079D; (b) W. Kim, R. Ryoo; Catal. Lett., 144 (2014) 1164-1169.